Superconductivity from Flat Dispersion Designed in Doped Mott Insulators

Masatoshi Imada[1] and Masanori Kohno[2]
[1]*Institute for Solid State Physics, University of Tokyo, Roppongi, Minato-ku, Tokyo 106-8666, Japan*
[2]*Mitsubishi Research Institute, Inc., Ootemachi, Chiyoda-ku, Tokyo, 100-8141, Japan*
(Received 23 June 1999)

Routes to enhance superconducting instability are explored for doped Mott insulators. With the help of insight for criticalities of metal-insulator transitions, geometrical design of lattice structure is proposed to control the instability. A guideline is to explicitly make flat band dispersions near the Fermi level without suppressing two-particle channels. In a one-dimensional model, numerical studies show that our prescription with finite-ranged hoppings realizes large enhancement of spin-gap and pairing dominant regions. We also propose several multiband systems, where the pairing is driven by intersite Coulomb repulsion.

PACS numbers: 74.20.Mn, 71.10.Li, 71.10.Fd, 71.27.+a

Basic properties of doped Mott insulators have been the subject of recent continued studies [1]. One of the goals of the studies is to find ways to design instabilities such as magnetism and superconductivity by controlling material parameters in a realizable way. It is desired to control the instabilities by utilizing the inherent character of the doped Mott insulators and the critical nature of metal-to-Mott insulator transitions. In this Letter, possible prescriptions to control the instabilities are proposed.

For single-band Hubbard and t-J models on a square lattice, simple scaling properties have been observed numerically near the transition from metals to Mott insulators [1–3], implying nontrivial and singularly momentum-dependent correlation effects, where single-particle excitations around some particular points as $(\pi, 0)$ and $(0, \pi)$ in the momentum space play crucial roles with the emergence of a flat dispersion [4]. This criticality extends to a 20%–30% doping range while it appears only below some fraction of the scale of the exchange interaction J. The flat dispersion was also numerically observed in the 2D Hubbard model in earlier works by Dagotto *et al.* [5], Bulut *et al.* [6], and Preuss *et al.* [7] in comparison to universally observed flat dispersions in angle-resolved photoemission data of the high-T_c cuprates [8,9]. Although the observed flat dispersion certainly results from a strong correlation effect with strong damping [3,5–7], the microscopic mechanism for the flat dispersion still waits for more complete understanding. Furthermore, its persistence in multiband or more complex systems has not been well studied.

In this Letter we discuss that promotion of the above scaling behavior by tuning the flat dispersion offers a way to control potential instabilities. We show that, even when a flat *band* dispersion is designed near the Fermi level by controlling lattice geometry and parameters, it enlarges the critical region under the suppression of single-particle coherence in the proximity of the Mott insulator mentioned above, thereby enhancing the instability. One might argue that if a flattened dispersion is designed, it simply makes the correlation effects relatively larger only through the change in the ratio to the effective bandwidth with the enhanced density of states. This is, however, not the whole story on the verge of itinerant and correlation-induced localized states. The metallic excitations are determined from the coherent one near the Fermi level, while the two-particle processes including the superexchange interaction J are rather determined mainly from a local, incoherent origin in the real space when the electron correlation is strong. It opens a possibility of enhancing the two-particle instability by suppressing the dispersion only near the Fermi level simultaneously keeping the amplitude of the two-particle processes large. By the suppression of only the single-particle coherence, two-particle processes work selectively and effectively since competition processes such as pair breakings and damping by the single-particle channel are suppressed. We find no particular dependence on dimensionality for this mechanism. This is, however, not possible in single-band models with nearest-neighbor hopping because the two-particle processes are not independent of the band dispersion near the Fermi level. We discuss below how the independent control can be made in more complex systems.

The flattened dispersion makes degenerate excitations and may cause various instabilities. In this context, we note that ferromagnetic instabilities by the flat band have been extensively studied [10–12]. However, we consider here only the cases with the singlet ground state at half filling, where the ferromagnetic instability is suppressed.

In 1D t-J models, the phase diagram in the parameter space of J/t and electron concentration n show a general tendency of stronger pairing instability, namely, the larger Tomonaga-Luttinger exponent K_ρ with spin gapped excitation for larger J/t, though the phase separation interrupts the enhancement [13–15]. Note that the pairing correlation is the most dominant if $K_\rho > 1$. The general tendency for enhanced pairing instability for large J/t also holds in 2D [16]. These are consistent with the mechanism we discussed above. We define the ordinary t-J model with the

three-site terms:

$$\mathcal{H} = -t\sum_{\langle ij\rangle}(\tilde{c}^{\dagger}_{i\sigma}\tilde{c}_{j\sigma} + \text{H.c.}) + J\sum_{\langle ij\rangle}\left(\mathbf{S}_i\cdot\mathbf{S}_j - \frac{1}{4}n_i n_j\right) - \frac{J}{4}\sum_{\langle ijk\rangle}(\tilde{c}^{\dagger}_{i\sigma}n_{j-\sigma}\tilde{c}_{k\sigma} - \tilde{c}^{\dagger}_{i\sigma}\tilde{c}^{\dagger}_{j-\sigma}\tilde{c}_{j\sigma}\tilde{c}_{k-\sigma} + \text{H.c.}), \quad (1)$$

where $\langle ij\rangle$ and $\langle ijk\rangle$ are nearest neighbors and $\tilde{c}^{\dagger}_{i\sigma}$ ($\tilde{c}_{i\sigma}$) creates (annihilates) electrons with the constraint to exclude the double occupancy. If the band dispersion is suppressed only near the Fermi level, the effective transfer decreases while J can be retained, mediated by the incoherent but dispersive part. This is indeed possible by introducing longer-ranged transfer. We introduce the 1D model with the third, fifth, and seventh neighbor transfers, t_3, t_5, and t_7, respectively and, for the exchange part, $J_i = J(t_i/t)^2$ accordingly, in addition to t and J [17]. We design flat noninteracting dispersion $\epsilon(q)$ by optimizing t_3, t_5, and t_7 to make terms up to the sixth order vanish in the wave number q around $q = \pm\pi/2$, the Fermi level at half filling. The spin-gap boundary and the exponent $K_\rho = \sqrt{\pi D n^2\kappa/4}$ were calculated by exact diagonalization of the Hamiltonian up to 16 sites, where the Drude weight D and the compressibility κ were calculated at filling n following the procedure in the literature [13–15]. For the spin gap boundary, we used the level crossing method for accurate estimates [15]. The results have practically no system size dependence implying a reliable estimate of the thermodynamic results. They show remarkable enhancement of both the pairing correlations and spin-gap region as in Fig. 1, where the phase separation is absent. It shows the mechanism we proposed is indeed effective. We have also examined other types of band modifications and confirmed that the above mechanism mainly determines the enhancements [17]. We have found that the corresponding Hubbard-type model with the same distant-ranged transfers also show a similar enhancement. However, the system sizes we could study are not large enough for reliable estimates of the thermodynamic limit. We note that the enhancement of pairing was also reported in the ladder model [18–20], when the Fermi level lies near the top (bottom) of bands, where a flattening is present. Our finding suggests one prescription, namely, looking for a tuned flatter dispersion arranged only near the Fermi level of the doped Mott insulator in quasi-one-dimensional conductors. Since the mechanism itself is not confined to quasi-one dimensionality, it opens various possibilities with rich physics along this line.

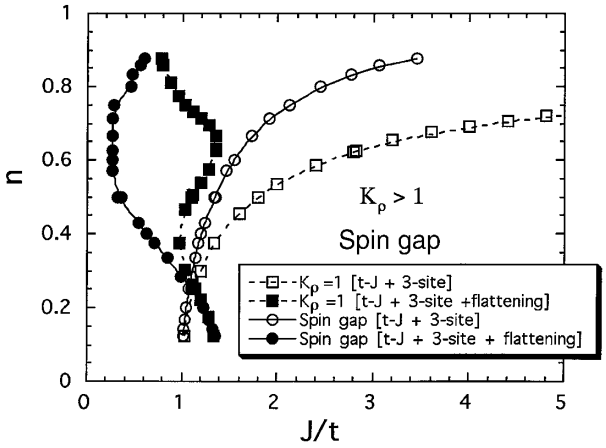

FIG. 1. Phase boundary of the spin-gap region (circles) and the contour lines (with squares) for the Tomonaga-Luttinger exponent $K_\rho = 1$. The case for the t-J model with the three-site term (open symbols) and that of the same model but with optimized dispersions by $t_3 = 0.6$, $t_5 = 0.2$, and $t_7 = 1/35$ and resultant J_3, J_5, and J_7, where $J_i = Jt_i^2$ (filled symbols).

Next, we analyze several multiband models with nontrivial band-flattening effects to get further insight into this issue and to provide hints for material synthesis. We introduce an extended Hubbard model,

$$\mathcal{H}_H = -t\sum_{\langle ij\rangle}(c^{\dagger}_{i\sigma}c_{j\sigma} + \text{H.c.}) - t'\sum_{\langle lm\rangle}(c^{\dagger}_{l\sigma}c_{m\sigma} + \text{H.c.}) + U\sum_i\left(n_{i\uparrow} - \frac{1}{2}\right)\left(n_{i\downarrow} - \frac{1}{2}\right) + \sum_{ij}V_{ij}n_i n_j, \quad (2)$$

where $c^{\dagger}_{i\sigma}$ ($c_{i\sigma}$) represent the creation (annihilation) operator of an electron at site i with spin σ. The lattices are defined below in Figs. 2–4 where t connects bonds with solid lines and t' connects broken bonds.

The first example belongs to a category of one-quarter depleted square lattice. Our model is described by the Hamiltonian (2) with the lattice structure illustrated in Fig. 2(a). When $t' = 0$, it reduces to a lattice considered by Lieb [10] if isolated spins on a quarter of lattice points are depleted. It has ferromagnetic ground state at half filling as Lieb proved. For $t' \neq 0$, however, the ground state becomes singlet at half filling due to the Lieb-Mattis theorem [21]. For smaller t'/t, the noninteracting dispersion shows flattening in the middle two bands among four in total. The two flattened dispersions are given by $E = \pm\sqrt{-\frac{1}{2}[\Xi - \sqrt{(\Xi + 2\sqrt{\Gamma})(\Xi - 2\sqrt{\Gamma})}]}$,

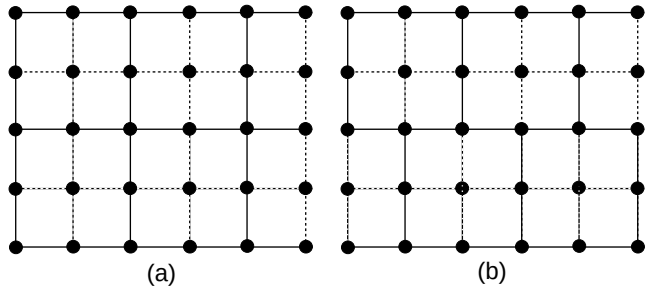

FIG. 2. (a) The first model with regular 1/4 depleted structure. (b) The second model with alternating 1/4 depleted structure.

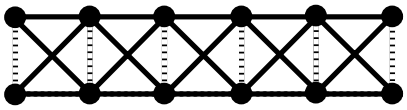

FIG. 3. The third model, ladder structure with diagonal transfer.

with $\Xi = (v^2 + w^2 - u^2)\cos(k_x - k_y) - 2u^2(\cos k_x + \cos k_y) - 3u^2 - v^2 - w^2$, $\Gamma = w^2u^2(\cos k_x - \cos k_y)^2$, $w = 2tt'/\sqrt{t^2 + t'^2}$, $u = \sqrt{t^2 + t'^2}$, $v = (t^2 - t'^2)/\sqrt{t^2 + t'^2}$. In the limit of $t' \to 0$, these two bands become completely flat. However flat the band becomes with small t'/t, the superexchange interaction on the solid bonds in Fig. 2(a) is unchanged. This lattice structure may favor triplet pairing instability near $t' = 0$ in contrast to the cases below, due to spin polarization of the flat nonbonding band.

The second model has a slightly different lattice from the case above as illustrated in Fig. 2(b). In this bipartite structure, the number of connected A and B sublattice points is equal, even at $t' = 0$, after removing isolated spins, where the ground state is singlet at half filling and the Mott insulating state with the antiferromagnetic order is expected in the thermodynamic limit. The flattening of the band is not complete in this case but still has an extended region of flat plateau.

The third example is illustrated in Fig. 3. The noninteracting bands consist of a dispersive bonding and completely flat antibonding bands. Under electron doping, carriers go into the flat band. Because of a strong frustration in contrast to the other cases, the magnetic correlation may be suppressed.

For the fourth system, the lattice structure is illustrated in Fig. 4. The square lattice structure in Fig. 4 is not important and the following argument applies to any other bipartite lattices if the three-site unit cell has the same structure. The band structure consists of antibonding, nonbonding, and bonding bands from high to low energies given by $\varepsilon_a = -tC_1 + \sqrt{(tC_1)^2 + 2t'^2}$, $\varepsilon_n = 0$, $\varepsilon_b = -tC_1 - \sqrt{(tC_1)^2 + 2t'^2}$, respectively, with $C_1 = \cos k_x + \cos k_y$ and an energy gap $\Delta_g \equiv -2t + \sqrt{4t^2 + 2t'^2}$. The noninteracting ground state at half filling is given by filled bonding and half-filled nonbonding bands.

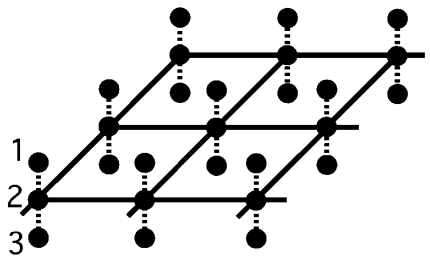

FIG. 4. The fourth model, decorated square lattice.

Below we discuss a general aspect of interaction effects more or less valid in all the above cases although we first take the fourth system as an example. For nonzero U, the flat band splits into upper and lower Hubbard bands. At half filling, the lower Hubbard band of this nonbonding band is filled, leading to the Mott insulator. Each cell is occupied by precisely one electron in the nonbonding orbital and an exchange interaction between these nonbonding electrons in the higher order in U may stabilize the antiferromagnetic order. In the perturbation expansion in U, we have mixing of antibonding components into the filled bonding band. However, in the perturbation, the number of nonbonding electrons at each cell can be changed only by two so that in all the cells precisely one nonbonding electron is kept up to the infinite order in U. Even away from half filling, when we once assign configuration for singly occupied and empty sites for nonbonding orbitals, they do not have dynamics, where macroscopic degeneracy remains. If the perturbation in U converges, the system remains insulating up to the doping concentration $\delta = 1/3$. Intracell but intersite interaction plays a similar role to U.

An important process in killing the insulating state arises from the intercell Coulomb repulsion $V_{|i-j|}$ $(i \neq j)$ between the ith and jth cells. For simplicity, we take V between the same sublattice points 1, 2, or 3 in Fig. 4. Other combinations play a similar role. Away from half filling, there appear empty and doubly occupied cells in the nonbonding orbitals. In the first order perturbation in $V_{|i-j|}$, a pair of electrons (holes) on the singly occupied nonbonding orbitals at sites i and j each is excited to the itinerant antibonding (bonding) band, where the excitation energy is roughly $2\Delta_g$. In the second order in V, a pair hopping from i, j cells to l, m cells occurs if l and m cells have initially no nonbonding electrons. Here we show the perturbation expansion up to the second order for the third model (Fig. 3):

$$\mathcal{H}_{\text{eff}} = \frac{1}{2}\sum_{i\delta} V_\delta n_{2,i} n_{2,i+\delta} - \sum_{\substack{i\delta \\ l\delta'}} V_\delta V_{\delta'} f_{il\delta\delta'} a^\dagger_{2,l+\delta',\sigma'} a^\dagger_{2,l,\sigma} a_{2,i,\sigma} a_{2,i+\delta,\sigma'},$$

$$f_{il\delta\delta'} = \sum_{kk'} \frac{\cos[k'(r_{l+\delta'} - r_{i+\delta})]\cos[k(r_l - r_i)]}{2t' - 4t(\cos k + \cos k')},$$

where $a^\dagger_{2,i,\sigma}$ creates a flat band electron at site i with spin σ. Similar effective Hamiltonians are derived for the other models.

From the second order process, the localized nonbonding electrons melt. It also induces superexchange-type magnetic interaction from the charge diagonal part. When V has some extended range, the superconducting order with the pairing form factor with this range may occur. The longer-ranged Coulomb interaction helps to inactivate the first order process in V. If $V_{|i-j|}$ does not depend on the combination (i, j), the first order process just gives a constant independently of the electron configuration. If $V_{|i-j|}$

is given by a screened form $\sim[\exp(-r_{ij}/R)/r_{ij}]V_0$ with the range R, the second order process generates averaged kinetic energy in the order $(V_0^2/\Delta_g)\delta^2(R/a)^2(t/\Delta_g)^2$ in 2D where a is the lattice constant. The average Coulomb repulsion energy generated from the first order process is roughly $V_0/\delta^{1/d}$ in d dimensions. Then the pairing interaction in the second order dominates for larger R. By a rough estimate inferred from the melting transition of the Wigner crystal [22], the dominance may well be realized for $R/a \gtrsim 3$ at $\delta \sim 0.1$ and $V_0/\Delta_g \sim \Delta_g/t \lesssim 1$. If this condition is not well satisfied, the charge ordering may compete with the superconductivity. A related multiband pairing mechanism was pointed out before [18,23], where the pair transfer through U drives the s-wave superconductivity. Although several other proposals for pairing in multiband models with V have been made [24,25], they are rather different from ours in the sense that our mechanisms come from (interband) pair transfers from flattened band near the Fermi level to dispersive channel. An artificial but helpful limit to understand the instability in our mechanism is the case of infinite-range transfer with the uniform amplitude $t/\sqrt{N}$ for system size N. In this case, the mean field solution with the order parameter $\Delta = \sum_k f(k)c_{k\sigma}c_{-k\sigma'}$ with $f(k) = \sum_{ij} V_{|i-j|}e^{ik|i-j|}/N$ becomes the correct description of the superconducting ground state, where the Hamiltonian has the form $\mathcal{H} = -\frac{1}{N}\Delta^\dagger\Delta\frac{t^2}{t'^3}$.

It is tempting to say that the above designed flattening seems to be an extreme limit of the high-T_c cuprates. In our models, the flat dispersion is separated from the dispersive bands. The high-T_c cuprates seem to be more similar to the fourth model at large U, where the dispersive (anti)bonding and the flat nonbonding bands coexist at the Fermi level.

It would be desired to seek materials which follow the prescription presented here. For the first and second systems, regular $1/4$ depletion of square lattice or substitution (for example, one-quarter of Cu ions with nonmagnetic ions on the CuO_2 lattice) may satisfy the requirement. It is interesting that this structure has some similarity to the charge ordered (or stripe) phase suggested in La-based high-T_c cuprates [26]. This connection provides a new view on the stripe problem [27]. The fourth model may be realized by three-layered structure with top and bottom layers designed to remove ligand atoms such as oxygen or substituted with different ligand atoms to suppress transfer through them in those planes.

One might argue that, with flat dispersions, impurity or phonon effects were serious in real materials. However, when the coherent single-particle excitations are suppressed, the localization effect is rather determined under the competition to the two-particle process. The localization effect is reduced if the two-particle hopping process is retained larger. Anyhow impurity and phonon effects near the Mott insulator in the present situation are important open problems left for future studies.

Our proposal to enhance the pairing instability is summarized: Design flat bands near the Mott insulator by retaining the preferred two-particle process. Because of the enhanced degeneracy and the suppression of the single-particle process, the doped system gets stronger instability in the two-particle process. We have numerically shown that this mechanism and prescription work in an example of 1D models with longer-ranged transfers. We have proposed several multiband lattices, where the intersite Coulomb repulsion generates such two-particle processes through interband pair hoppings. Because the coherent single-particle process is absent, small intersite interaction immediately corresponds to the strong coupling limit of the pairing where the Fermi liquid state does not exist.

The authors thank H. Asakawa and H. Tsunetsugu for useful discussions. This work is supported by a Grant-in-Aid for "Research for the Future" Program from the Japan Society for the Promotion of Science under the Project No. JSPS-RFTF97P01103.

[1] For a review, see M. Imada, A. Fujimori, and Y. Tokura, Rev. Mod. Phys. **70**, 1039 (1998).
[2] M. Imada, J. Phys. Soc. Jpn. **64**, 2954 (1995).
[3] M. Imada, *Physics and Chemistry of Transition Metal Oxides*, edited by H. Fukuyama and N. Nagaosa (Springer-Verlag, Berlin, 1999), p. 120.
[4] F. F. Assaad and M. Imada, Eur. Phys. J. B **10**, 595 (1999).
[5] E. Dagotto, Rev. Mod. Phys. **66**, 763 (1994); A. Nazarenko *et al.*, Phys. Rev. B **51**, 8676 (1995).
[6] N. Bulut, D. J. Scalapino, and S. R. White, Phys. Rev. B **50**, 7215 (1994).
[7] R. Preuss *et al.*, Phys. Rev. Lett. **79**, 1122 (1997).
[8] K. Gofron *et al.*, Phys. Rev. Lett. **73**, 3302 (1994).
[9] Z.-X. Shen and D. S. Dessau, Phys. Rep. **253**, 1 (1995).
[10] E. Lieb, Phys. Rev. Lett. **62**, 1201 (1989).
[11] A. Mielke, J. Phys. A **24**, L73 (1991).
[12] H. Tasaki, Prog. Theor. Phys. **99**, 489 (1998).
[13] M. Ogata *et al.*, Phys. Rev. Lett. **66**, 2388 (1991).
[14] B. Ammon, M. Troyer, and H. Tsunetsugu, Phys. Rev. B **52**, 629 (1995).
[15] M. Nakamura, K. Nomura, and A. Kitazawa, Phys. Rev. Lett. **79**, 3214 (1997).
[16] E. Dagotto *et al.*, Phys. Rev. B **49**, 3548 (1994).
[17] M. Kohno and M. Imada (unpublished).
[18] K. Yamaji and Y. Shimoi, Physica (Amsterdam) **222C**, 349 (1994).
[19] K. Kuroki, T. Kimura, and H. Aoki, Phys. Rev. B **54**, R15 641 (1996).
[20] R. M. Noack, N. Bulut, D. J. Scalapino, and M. G. Zacher, Phys. Rev. B **56**, 7162 (1997).
[21] E. Lieb and D. Mattis, Phys. Rev. **125**, 164 (1962).
[22] M. Imada and M. Takahashi, J. Phys. Soc. Jpn. **53**, 3770 (1984).
[23] J. Kondo, Prog. Theor. Phys. **29**, 1 (1963).
[24] C. Varma, Solid State Commun. **62**, 681 (1987).
[25] E. B. Stechel *et al.*, Phys. Rev. B **51**, 553 (1995).
[26] J. M. Tranquada, Nature (London) **375**, 561 (1995).
[27] M. Imada (unpublished).